Journal of Geology & Geophysics

OPEN ACCESS Freely available online

Research Article

Empirical Relationship between Gravimetric and Mechanical Properties of Basement Rocks in Ado-Ekiti, Southwestern Nigeria

Ajayi CA[1]*, Akintorinwa OJ[2] and Ademilua LO[1]

[1]*Department of Geology, Ekiti State University Ado Ekiti (EKSU)*

[2]*Department of Applied Geophysics, Federal University of Technology Akure (FUTA)*

ABSTRACT

Gravimetric and mechanical parameters of Basement rocks in Ado-Ekiti, South-western Nigeria were correlated for engineering foundation studies with the aim of establishing an empirical relationship between the two parameters. Field operations revealed Charnockite, Migmatite, Granite Gneiss and Quartzite as principal basement rocks in the study area. Fresh rock samples were taken from thirty (30) locations cutting across the geology of the study area. Simple pendulum principle and Archimede's principles were employed to determine the gravity and the specific gravity of the rock specimens repectively. The mechanical analyses (uniaxial compressive strength, shear strength, Young's modulus, Bulk modulus and Poisson's ratio) for the thirty rock samples were determined employing standard method. This is applicable to all engineering foundation studies to determine the compence of such areas for engineering developments. The engineering studies revealed the reliability, stiffness, soundness and resistance of the subsurface rocks to the prevailing overhead loads.

The results indicated that the gravity and specific gravity values ranged from 935055.46 mgal to 1038167.647 mgal and 2.61 to 2.83 respectively. The values of Uniaxial Compressive Strength (UCS), Young's modulus (E), Shear modulus (μ), Bulk modulus (K) and Poisson's ratio (V) ranged from 49–107 mpa, 1003–3321 mpa, 416–1310 mpa,707–2728 mpa and 0.232-0.316 respectively. The cross plots of the mechanical parameters with gravity and specific gravity showed good correlation with coefficient of correlation (R) ranging from 0.52 to 0.84 and 0.52 to 0.81 respectively. Results validation exercise also indicated that some of the Uniaxial Compressive Strength and Poisson's ratio have good representation in the derived empirical equation with the two geophysical parameters in this study. The established relationship between the gravimetric and the mechanical parameters revealed that; the mechanical strength of rock is a function of the gravitational pull effect on the rocks and that migmatitic and granitic rocks possessed more mechanical strength than the gneissic and quarzitic rocks that characterised the study area. Some of the equations generated has been found reliable and useful in the determination of the mechanical properties. The physical methods adopted being faster, cheaper, proven and more comprehensive would solve some engineering problems in examining the engineering properties of these basement rocks related terrains.

Keywords: Gravity; Specific gravity; Correlation; Physical properties; Mechanical strength; Young's modulus; Bulk modulus; Shear modulus; Poisson's ratio; Rocks; Empirical relationship

INTRODUCTION

Geophysical methods have been embraced over the years by most technologically advanced countries as a vital tool in engineering site investigations for estate development and management. Geophysics has been used to solve many civil engineering problems that had hitherto proved costly, complex or unattainable by other civil engineering methods. Methods employed in geophysical investigation are considered to be non-destructive, time-saving, less-expensive and very effective in site probing for engineering studies [1]. Over the years, geophysical prospecting method coupled with geotechnical analysis has been successfully helpful in determining the condition of the subsurface for civil engineering investigation [2]. Mineralogical alteration of rocks contributes to changes in their physical and mechanical properties [3]. The finer-grained rocks are usually stronger than coarse grained varieties as a result of higher grain to grain contacts in fine-grained samples [4].

***Correspondence to:** Ajayi Christopher Ayodele, Department of Geology, Ekiti State University, Nigeria, Tel: +2348033505138; E-mail: christopher.ajayi@eksu.edu.ng

Received: October 23, 2019**; Accepted:** December 21, 2019**; Published:** January 2, 2020

Citation: Ajayi CA, Akintorinwa OJ and Ademilua LO (2020) Empirical Relationship between Gravimetric and Mechanical Properties of Basement Rocks in Ado-Ekiti, Southwestern Nigeria. J Geol Geophys 9:470. 10.35248/2381-8719.19.9.470

Adapted civil engineering methods for rock strength investigation consume time and money which can be reduced drastically by applying specific geophysical method. Therefore, establishing empirical relationships between the geophysical properties of rocks and their mechanical properties, can serve as complementary measure in determining the mechanical strength of rock from the geophysical data. This study is aimed at evaluating the empirical relationship between geophysical parameters (gravity) and some mechanical properties of Basement rocks in Ado-Ekiti.

Ado-Ekiti been the capital of Ekiti-State is witnessing rapid structural development such as fly-over bridges, high rising building etc. The durability and stability of these structures depend on the mechanical strength of the underlying rock/subsoil. The conventional ways of determining the mechanical properties of the parent rocks which weathered into subsoil is time consuming and not cost effective. These challenges are not limited to Ado-Ekiti as construction activities are on continuous basic. Hence, this study focused on establishing empirical relationship between gravity and some mechanical properties of basement rocks. Mechanical properties of basement rocks can be evaluated directly from the empirical equation thereby reducing cost and time waste.

Location of study

Ado-Ekiti lies between Longitude 736000 to 754000 and Latitude 832000 to 854000 Universal Traverse Mecartum (Figure 1), covering a total area of 346.5 km^2. The study area is accessible through major and minor roads (Figure 1). Ado-Ekiti and its environs are dominated by crystalline rocks (Figure 2) which consist mainly of migmatite-gneiss-quartzite complex, older granites, quartzite, charnockites, and fine to medium grained granites [5]. In the study area, there is a close association between the charnockites and granitic rocks due to their field relationship as documented in the Basement complex rocks of Nigeria [6]. Migmatite covers over 50% of the study area (Figure 1 and Figure 2) which host intrusion of other rocks. Migmatite rock exposures occur as highly denuded hills of essentially fine texture while the pegmatites are very coarse-grained with phenocrysts of feldspar over 2500 mm in length, usually of granitic composition and forming at a late stage of crystallization. In the study area, the migmatite-gneiss rocks

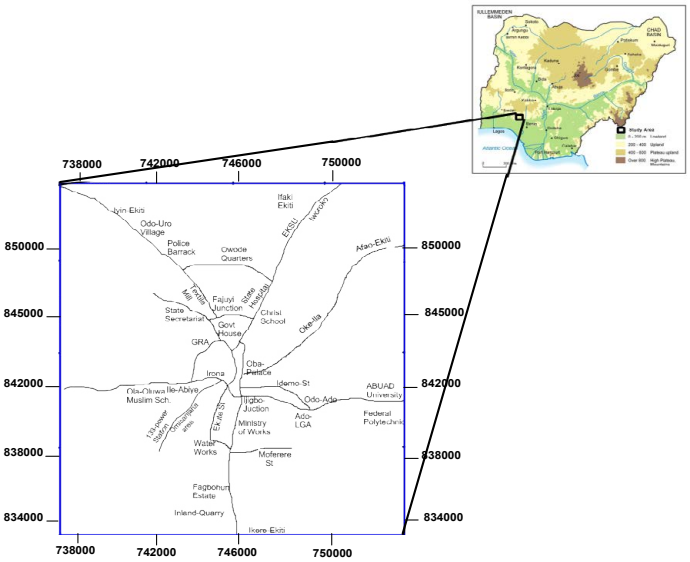

Figure 1: Map of Nigeria showing relief, morphology and the road networks within the study area.

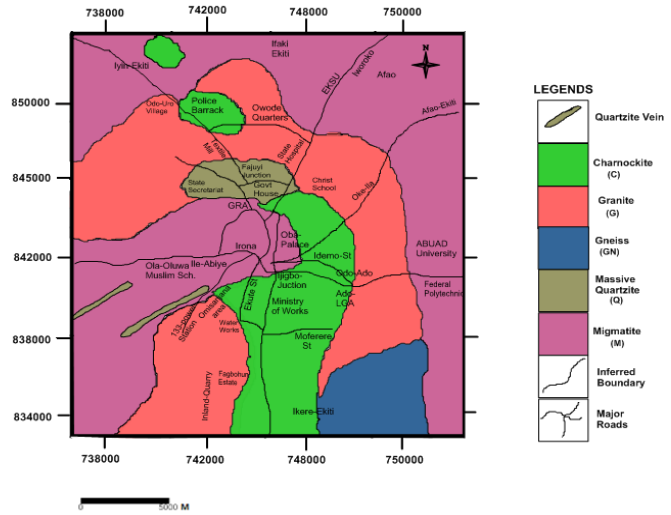

Figure 2: Geology map of Ado-Ekiti study area [4].

composed of a mafic portion, made up of biotite, hornblende and opaque minerals while the felsic portion is quartzofeldspatic [7].

The charnockitic rocks outcrops within the study area are massive, dark-greenish in colour with medium to coarse grained texture. The charnockites in Ado-Ekiti fall within those that occur along the margins of Older Granites bodies especially the porphyritic granites [6]. Petrological studies reveal that charnockite contains quartz, alkali feldspar, plagioclase and biotite as major mineral. The charnockitic rocks outcropped as pavement and oval or semi-circular hills of between five and ten meters (10 m) high with a lot of boulders at some outcrops. They are generally massive, dark-greenish in colour with medium to coarse grained texture. The fresh outcrops with little or no sign of weathering have a lot of quartz, aplite and pegmatite intrusions occurring in it [7]. The basement rocks are believed to have evolved as a result of at least four major orogenic cycles of deformation, metamorphism and re-mobilization corresponding to the Liberian (2700Ma), Eburnean (25000Ma), Kiberian (1100Ma) and lastly, the Pan-African Orogeny (650Ma). The three first cycles were characterized by intense deformation and isoclinal folding accompanied by regional metamorphism, which was further followed by extensive migmatization, granitisation, and gneissification which produced syntectonic granites and homogenous gneisses [8]. Late tectonic emplacement of granites and granitoids are associated with contact metamorphism which accompanied end stages of the last deformation.

The Older Granites comprise of felsic and mafic minerals. The felsic minerals include quartz, orthoclase, plagioclase feldspar and muscovite while the mafic group comprise of the black coloured biotite and the dark green to black hornblende of the amphibole group [9]. The granites are distinguishably unique because of their visible minerals, lack of foliation, fine-medium grained texture and compact interlocking crystals that developed during the crystallisation of magma [7]. A plutonic complex containing both charnickitic and Non-charnockitic granite rocks (Older Granites) occurs within the amphibolite facies rocks of gneisses and migmatites in Ado Ekiti, Southwestern Nigeria [10]. Mineralogical alteration of rocks contributes to changes in their physical and mechanical properties [3]. Geophysical methods were employed over the years to investigate geologic structural features, Basement disposition, delineation of rock types, depth to competent bedrock etc. Remote sensing and aeromagnetic as geophysical method can be integrated to delineate geologic structural features and hydrothermal

alterations [11]. Aeromagnetic data was also used for enhancing geologic features applying co-occurrence matrices [12]. In their work were able to evaluate brittleness of rock using ultrasonic pulse velocity [13]. Rock mechanics properties were characterized using correlated laboratory test and numerical interpretations of well logs [14]. This research is aimed at evaluating the empirical relationship between gravity as a physical parameter and some mechanical properties of Basement rocks within Ado-Ekiti, Southwestern Nigeria. To achieve this aim, the objectives of the study are: To determine the mechanical properties, density, specific gravity of the sampled rocks, to determine the gravity values of each rock type employing simple harmonic motion (simple pendulum principle) method in the laboratory, use above to establish an empirical equations from which mechanical parameters can be determined using the measured gravity values; and validate the established empirical equations.

METHODS OF STUDY

This research employed the use of gravity geophysical method vis-à-vis mechanical method involving determination of the uniaxial compressive strength, Young's modulus, Bulk modulus, Poisson's ratio and shear modulus of each of the rock sample. The specific gravity and gravity were determined and correlated with each of the mechanical properties.

Gravity values determination

Simple harmonic motion of Galile Galileo principle was adopted to determine the gravity of each sampled rock [15]. The materials used for the determination of the Gravity values are: swing rope, roof clip, electric weighing balance, meter rule, hammer and stop-watch. Thirty samples from the different rock types (charnockite, migmatite, granite, gneiss and quartzite) were taken from different locations within the study area (Figure 3). Six samples of each rock unit with weights varying from 3-4 kg were taken with the aid of sledge hammer. The samples were further broken into smaller sizes of equal weight of approximately 60 gm. The pendulum rope

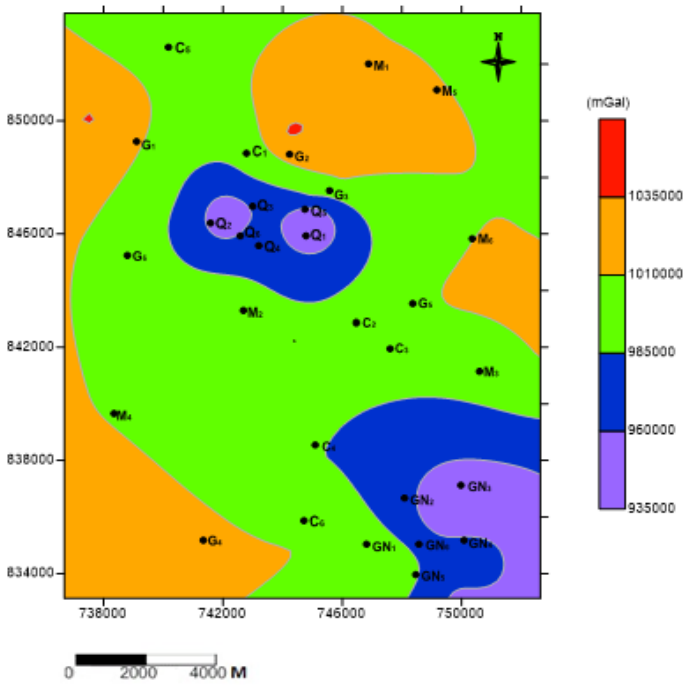

Figure 3: Gravity values map of the study area.

was hung to the ceiling of the laboratory with the aid of the clips nailed against the ceiling. The height of the ceiling to the floor was 3.6 m. Each of the samples was set at lengths of 3.2 m tied on the rope tightly. The sample on the pendulum was held at an angle of about 60^0 to the perpendicular axis against the ceiling. The pendulum was set in motion until it completes fifty (50) to and fro oscillations. Time taken to make fifty (50) oscillations was recorded twice as 't_1' and 't_2' in seconds. An average time-taken (t) for fifty (50) oscillations was recorded in seconds, while the period (T) was calculated by dividing the total time (t) for the fifty oscillations by 50 (no of oscillations) (Plate 3.1). The square of the period (T^2) was also calculated. The length 'L' of the rope was further varied to 3.0 m, 2.8 m, 2.6 m, 2.4 m and 2.2 m with the sample attached.

The square of the period (T^2) was also calculated at the varying lengths. Values of swing rope length (L) were plotted against square of period (T^2). The gradient was then determined from the plot. Using the Galileo equation of simple pendulum motion, which states "The period (T) for a simple pendulum does not depend on the mass or the initial angular displacement, but depends only on the length (L) of the string and the value of the gravitational field strength (g)," where;

$$T = 2\pi\sqrt{L/\mathrm{g}} \quad (1)$$

$$T = 2\pi\sqrt{(\mathrm{n}-L)/\mathrm{g}} \quad (2)$$

Where, T = period,

L=length of the rope,

h=distance between the floor and the sample before swinging and

g=acceleration due to gravity.

Square both sides of equation 1:

$$T^2 = 4\pi^2(\mathrm{h}-\mathrm{L})/g \quad (3)$$

$$T^2 = 4\pi^2 h/g - 4\pi^2 L/g \quad (4)$$

$$T^2 = -4\pi^2 L/g + 4\pi^2 h/g \quad (5)$$

Where $-4\pi^2/g$ is the gradient (m) of the linear graph. The negative sign signifies deceleration during the pendulum motion. The values of gradient (m) calculated from the graph was equated with the gradient $T^2 = -4\pi^2/g$ of the linear equation (equation 5) without the negative sign to obtain the gravity (g) values.

Specific gravity determination

The densities of samples of the thirty rock samples were determined in the laboratory by adopting the bulk density and buoyancy methods. Small sizes of the sample were first weighed on the weighing balance to determine the weight in air 'Wa', which ranges from 26 gm to 79 gm. The weight of the beaker half-full with water was also weighed as 'W_b'. Rock sample was then hung on the clip of the tripod stand with aid of the thread and suspended into the water and then weighed as 'Wc'. Weight of the sample in water 'Ww' was determined by subtracting the weight of the beaker with water 'W_b' from weight of the beaker with water and the suspended sample 'Wc'. Bulk density (ρ) is then determined by:

$$\rho = W_a/W_a - W_w \quad (6)$$

The Specific gravity of each sample was then calculated by multiplying the bulk density (ρ) obtained with the density of water (ρ_w) which is equal to 0.9986 g/cm^3. Then,

$$SG=\rho \times \rho_w \quad (7)$$

$$SG=\rho \times 0.9986 \quad (8)$$

By applying the buoyancy method, the weight of the rock sample in air was determined and the volume of water displaced (Vs) in the beaker was measured. The bulk density of the rock sample was calculated by dividing the weight of the sample in air (Wa) by the displaced volume of water (Vs) and multiplying by the density of water (0.9986 g/cm^3).

$$\rho = W_a / V_s \quad (9)$$

$$SG = \rho \times \rho_w \quad (10)$$

$$SG = \rho \times 0.9986 \quad (11)$$

Determination of mechanical properties of rocks

Fresh rock samples of rocks were collected from outcrop in each of the locations within the study area (Figure 2). A total of thirty (30) rock samples were taken to the laboratory and cut with the aid of rock cutting machine into cuboid shape of 2 cm by 1.5 cm by 6 cm dimension. Determination of the Uniaxial Compressive Strength (UCS) entails measuring and recording the actual dimension of each of the prepared rock sample. Then each of the prepared samples was mounted on the Uniaxial Compressive Strength machine. The dial gauge and the load gauge of the machine were standardized to zero reading prior to use.

The dial gauge reads the strain on the rock sample; while the load gauge reads the stress. The coarse adjustment load roller is then turned until the rock breaks (as a sign of failure). The plunger was made to touch the surface of the specimen, and the load and penetration measuring dial was set to zero. The plunger was made to penetrate the prepared rock sample at constant rate of 1 mm per minute. The deformation readings were taken at every 25 deformation dial reading until the compacted rock specimen breaks or deforms. The sample stress and strain were computed and the normal stress was plotted against the axial strain. The peak of the resultant curve was taken as the Uniaxial Compressive Strength (MPa).

From the uniaxial compression test curve, Mohr circle was generated with the aid of Microsoft-Excel equation. Shear stress and the corresponding strain were obtained from the Mohr-circle and uniaxial compression test curve to obtain the shear modulus.

Employing Mavko *et al.*, (2003) formula, Bulk Modulus (k) was obtained as stated in equation 12.

$$K = E_\mu / 3(3_\mu - E) \quad (12)$$

Where, E =Young's Modulus, μ =Shear Modulus and k =Bulk Modulus

Poisson's Ratio (v) was obtained by applying Mavko formula that relate the Poisson's Ratio (**V**) with the Young's Modulus (E) and the Shear Modulus (μ) in equation 13), i.e.

$$V = E/2_\mu - 1 \quad (13)$$

RESULTS AND DISCUSSION

Gravity results

The gravity values map generated from the laboratory data is as shown in Figure 3. Table 1 shows the values of the gravity for each of the sample analyzed. The gravity distribution within the study area ranges from 935000-104000 mGal (Figure 3). Relatively low gravity values (<985000 mGal) were observed at the central and the southeastern part of the study area. This falls within the region underlain by gneiss and quartzite rock. However, relatively high gravity values (>985000 mGal) were observed within the areas underlain by migmatite, charnockite and granite. This shows that migmatite, granite and charnockite are denser than other rock types within the study area. This may reflect in their weathering-end. The gravity values reflect how dense the subsurface basement rocks are which can be used as a parameter to determine their durability in withstanding surface loads from engineering structures (Table 2).

Specific gravity

Table 3 shows the result of the specific gravity test within the study area. Specific gravity values in the study area range from 2.59–2.84 (Figure 4). It shows relative low values (<2.71) in the areas mostly

Table 1: Gravity values of the sampled rocks.

Sample	Rock Type	Gravity (m/s^2)	Gravity (Gal or cm/s^2))	Gravity (m gal)
C1	Charnockite	9.956706274	995.6706274	995670.6274
C2	Charnockite	10.03359008	1003.359008	1003359.008
C3	Charnockite	9.975060808	997.5060808	997506.0808
C4	Charnockite	9.845036712	984.5036712	984503.6712
C5	Charnockite	9.885468575	988.5468575	988546.8575
C6	Charnockite	10.09229453	1009.229453	1009229.453
M1	Migmatite	10.0832778	1008.32778	1008327.78
M2	Migmatite	10.03180638	1003.180638	1003180.638
M3	Migmatite	10.09538131	1009.538131	1009538.131
M4	Migmatite	10.10934145	1010.934145	1010934.145
M5	Migmatite	10.04737144	1004.737144	1004737.144
M6	Migmatite	10.09538949	1009.538949	1009538.949
G1	Granite	10.36587525	1036.587525	1036587.525
G2	Granite	10.38167647	1038.167647	1038167.647
G3	Granite	10.1116705	1011.16705	1011167.05
G4	Granite	10.13632045	1013.632045	1013632.045
G5	Granite	10.11840488	1011.840488	1011840.488
G6	Granite	10.09719608	1009.719608	1009719.608
GN1	Gneiss	10.00284649	1000.284649	1000284.649
GN2	Gneiss	9.386061732	938.6061732	938606.1732
GN3	Gneiss	9.48774606	948.774606	948774.606
GN4	Gneiss	9.547127686	954.7127686	954712.7686
GN5	Gneiss	9.495718839	949.5718839	949571.8839
GN6	Gneiss	9.83694611	983.694611	983694.611
Q1	Quartzite	9.350734021	935.0734021	935073.4021
Q2	Quartzite	9.772938667	977.2938667	977293.8667
Q3	Quartzite	9.76791535	976.791535	976791.535
Q4	Quartzite	9.728411191	972.8411191	972841.1191
Q5	Quartzite	9.904528559	990.4528559	990452.8559
Q6	Quartzite	9.3505546	935.05546	935055.46

Table 2: Classification of gravity values of the subsurface formation and their implication on the surface engineering structure.

Description	Gravity (m gal)	Implication on Surface Structure
Very High	>1035000	Very Dense
High	1010000 - 1034999	Dense
Medium High	985000 - 1009999	Rarely Dense
Low	9600000 - 984999	Low Weight
Very Low	< 960000	Very Low Weight

Table 3: Specific gravity values in the study area.

S/N	Sample	Rock Type	Density In g/cm^3	Specific Gravity From Density (G1)	Specific Gravity From Buoyancy (G2)	Average Specific Gravity (G)
1	C1	Charnockite	2.594	2.619	2.6153	2.7679
2	C2	Charnockite	2.663	2.706	2.7022	2.7059
3	C3	Charnockite	2.649	2.701	2.6972	2.7143
4	C4	Charnockite	2.612	2.702	2.6982	2.6552
5	C5	Charnockite	2.624	2.651	2.6477	2.7234
6	C6	Charnockite	2.659	2.679	2.6756	2.6954
7	M1	Migmatite	2.831	2.827	2.8519	2.8395
8	M2	Migmatite	2.821	2.8171	2.7778	2.7976
9	M3	Migmatite	2.82	2.8156	2.7914	2.8035
10	M4	Migmatite	2.803	2.7994	2.8412	2.8203
11	M5	Migmatite	2.827	2.8233	2.8344	2.8289
12	M6	Migmatite	2.849	2.8447	2.7654	2.8051
13	G1	Granite	2.664	2.6603	2.6552	2.6578
14	G2	Granite	2.673	2.6693	2.7	2.6847
15	G3	Granite	2.651	2.6473	2.5882	2.6178
16	G4	Granite	2.648	2.6444	2.5537	2.5991
17	G5	Granite	2.657	2.6531	2.7554	2.7043
18	G6	Granite	2.659	2.6549	2.5965	2.6257
19	GN1	Gneiss	2.65	2.6463	2.6957	2.671
20	GN2	Gneiss	2.64	2.6433	2.6714	2.6574
21	GN3	Gneiss	2.658	2.6544	2.6465	2.6505
22	GN4	Gneiss	2.654	2.6498	2.6776	2.6637
23	GN5	Gneiss	2.649	2.6448	2.6934	2.6691
24	GN6	Gneiss	2.66	2.6558	2.6891	2.6745
25	Q1	Quartzite	2.594	2.5904	2.619	2.6047
26	Q2	Quartzite	2.663	2.6596	2.6316	2.6456
27	Q3	Quartzite	2.649	2.6453	2.6667	2.656
28	Q4	Quartzite	2.612	2.6083	2.6154	2.6119
29	Q5	Quartzite	2.624	2.6208	2.6332	2.627
30	Q6	Quartzite	2.659	2.6555	2.6566	2.6561

underlain by quartzite and gneiss. However, relatively high values (>2.71) of specific gravity are observed around the areas underlain predominantly by charnockites, migmatite and granite. Specific gravity is also a function of weight or density which is also a factor to be considered for a sustainable foundation rock or soils (Table 4).

Mechanical Properties

Uniaxial compressive strength (ucs): The results of the mechanical properties of rocks underlain the study area are shown in Table 5. The distribution of the Uniaxial Compressive Strength within the study area is as shown in Figure 5. The map indicates low Uniaxial Compressive Strength values (40–70 MPa) within zones that are characterized by charnockite, quartzite and gneiss rocks. The areas underlain by granite and migmatite show relatively high Uniaxial

Table 4: Classification of specific gravity values of the subsurface formation and their implication on the surface engineering structure.

Description	Specific Gravity	Implication on Surface Structure
Very High	>2.83	Very Dense
High	2.77–2.83	Dense
Medium High	2.71–2.76	Moderately Dense
Low	2.65–2.70	Low Weight
Very Low	<2.65	Very Low Weight

Table 5: Results of the rock mechanical test in the study area.

S/N	Sample	Rock Type	Uniaxial Compressive Strength (MPa)	Young Modulus (MPa)	Poisson's Ratio	Bulk Modulus (MPa)	Shear Modulus (MPa)
1	C1	Charnockite	65.5	1709.72	0.251	1144.39	683.341
2	C2	Charnockite	74.2	2411.66	0.262	1688.837	955.491
3	C3	Charnockite	65.6	1881.57	0.252	1264.495	751.426
4	C4	Charnockite	63.4	1668.47	0.248	1103.485	668.458
5	C5	Charnockite	63.5	1677.11	0.262	1174.446	664.465
6	C6	Charnockite	77.7	2528.29	0.273	1856.306	993.044
7	M1	Migmatite	76	2172	0.271	1580.786	854.445
8	M2	Migmatite	72.3	3321.83	0.267	2376.13	1310.904
9	M3	Migmatite	81.5	2370.4	0.288	1863.522	920.186
10	M4	Migmatite	91.3	2677.6	0.297	2198.357	1032.228
11	M5	Migmatite	71.2	1791.5	0.247	1180.171	718.324
12	M6	Migmatite	87.1	2677.6	0.288	2105.031	1039.441
13	G1	Granite	107.3	2766.08	0.307	2388.67	1058.179
14	G2	Granite	107.8	2364.78	0.316	2142.011	898.473
15	G3	Granite	92.1	2070.89	0.292	1659.367	801.428
16	G4	Granite	93.8	3105.3	0.294	2512.379	1199.884
17	G5	Granite	104.8	2705.6	0.314	2424.373	1029.528
18	G6	Granite	90.2	3359.05	0.294	2717.678	1297.933
19	GN1	Gneiss	69	1044.68	0.254	707.778	416.539
20	GN2	Gneiss	49.3	1311.49	0.242	847.216	527.975
21	GN3	Gneiss	55.8	1757.78	0.245	1148.876	705.936
22	GN4	Gneiss	57.8	2181.23	0.251	1459.993	871.795
23	GN5	Gneiss	57	1063.03	0.252	714.402	424.533
24	GN6	Gneiss	63.2	1426.46	0.259	986.487	566.505
25	Q1	Quartzite	48.8	2076.1	0.235	1305.723	840.526
26	Q2	Quartzite	59.8	1767.34	0.232	1099.092	717.265
27	Q3	Quartzite	59.4	1766.75	0.233	1102.84	716.444
28	Q4	Quartzite	58.3	2044.28	0.234	1280.877	828.314
29	Q5	Quartzite	40.2	1539.25	0.228	943.168	626.73
30	Q6	Quartzite	47.9	2091.88	0.235	1315.648	846.915

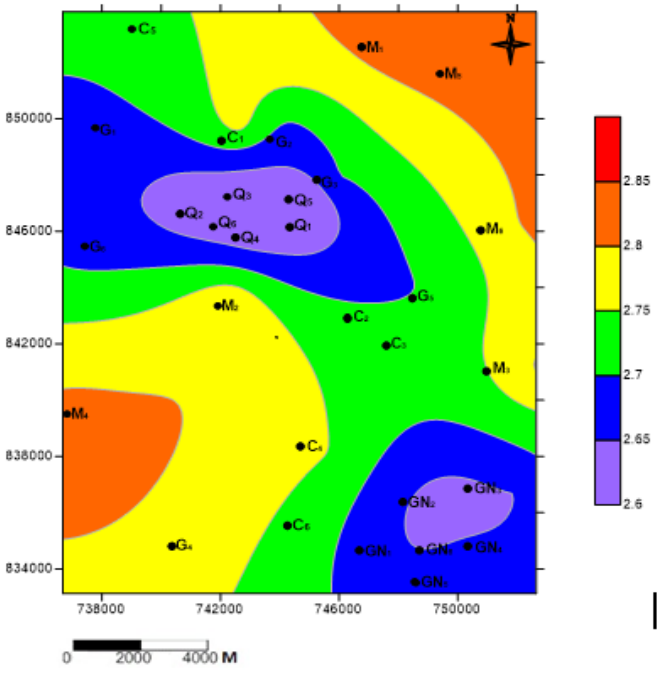

Figure 4: Specific gravity map of the study area.

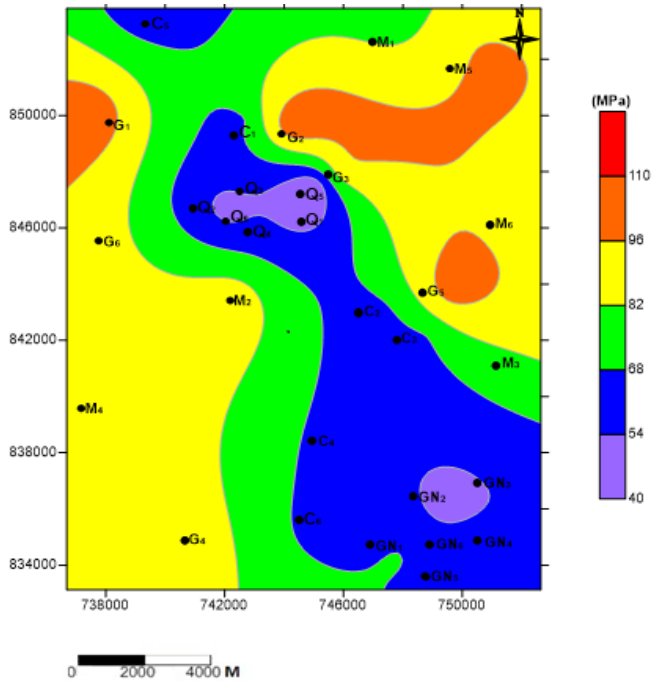

Figure 5: Uniaxial compressive strength map of the study area.

Compressive Strength values (85–115 MPa). This indicates that, the weathering products of granite and migmatite may be of high strength than other rocks in the study area. The UCS can be used to determine the soundness of the subsurface rock for the purpose of engineering constructions (Table 6).

Young's modulus: Figure 6 shows Young's modulus map of the study area. The Young's modulus of the study area ranges from 1000–3400 MPa. Relatively low values (1000–2120 MPa) were observed around the area characterized by gneiss, quartzite and charnockite rocks. Relatively high Young's composed of granite and migmatite rocks.

This is confirming the high strength nature of migmatite and granite relative to other rock types in the study area. Young's Modulus determines the stiffness of the subsurface rock against the overhead load of the engineering structures (Table 7). Highly yielding rock formation with low Young's Modulus values are susceptible to imminent failure if proper engineering precautions are not well envisaged.

Shear modulus: Shear modulus is parameter that can be used to determine the resistance of material to shearing stresses. The shear modulus distribution in the study area is as shown in Figure 7. It ranges from 400–1350 MPa. The map shows relatively low values (400–860 MPa) within the areas underlain by quartzite and charnockite rocks. The area characterised with relatively high shear

Table 6: Classification of UCS of the subsurface formation and their implication on the surface engineering structures.

Description	Ucs Strenght (mpa)	Implication (foundation)
Very High	>100	Sound
High	85-99	Good for any structure
Moderately High	70-84	Good for any structure except large dam
Low	45-69	Variable
Very Low	<44	Unreliable

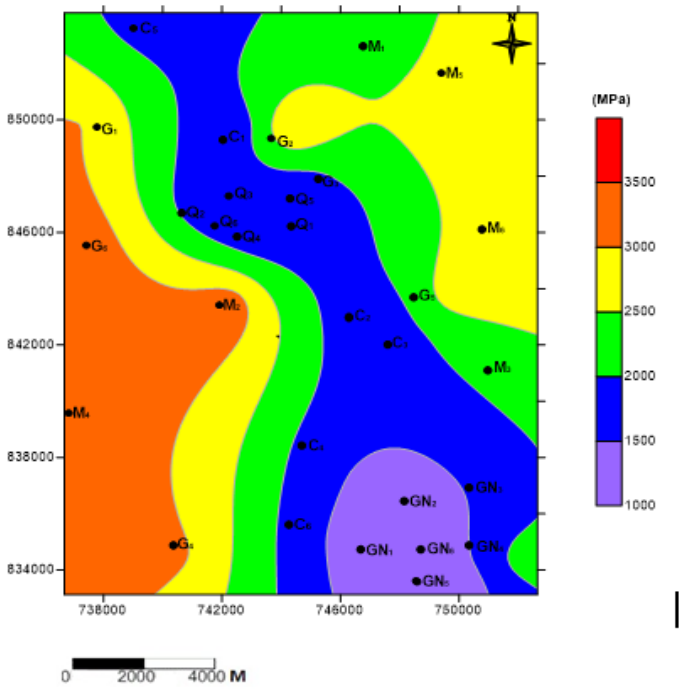

Figure 6: Young's modulus map of the study area.

Table 7: Classification of Young's modulus of the subsurface formation and their implication on the surface engineering structures.

Description	Young's Modulus (mpa)	Implication on Surface Structure
Very High	>3240	Very Stiff
High	2680–3239	Stiff
Medium high	2120–2679	Medium Stiffness
Low	1560–2119	Low Stiffness
Very Low	<1559	High Yielding

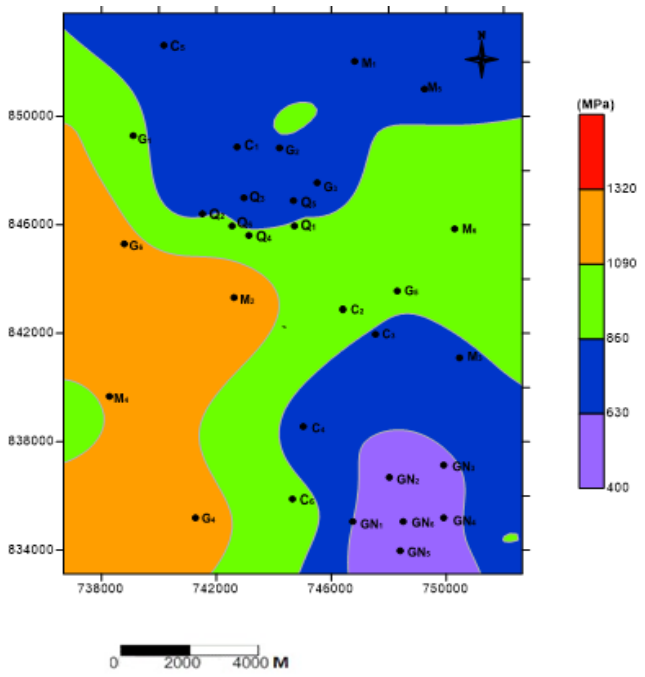

Figure 7: Shear modulus map of the study area.

mdulus values (>860 MPa) are underlain by migmatite and granite rocks. The shear modulus of the study shows that, area underlain by charnockite, gneiss and quartzite are of comparatively of lower strengths than areas underlain by migmatite and granite rocks. Shear Modulus reveals the resistance the underlying rocks possess against the shearing forces (Table 8).

Bulk modulus: Bulk modulus is a geomechanical parameter that best represents the mechanical behavior of rock mass. It describes how resistive a material can be to compressive forces. The bulk modulus (k) map of the study area is as shown in Figure 8. The value ranges from 700 to 2900 MPa. The map reveals relatively low values (<1700 MPa) of bulk modulus within the areas that are underlain by quartzite, charnockite and gneissic rocks. The relatively high values (>1700 MPa) were observed within the underlain by migmatite and granitic rocks. This also confirmed the high strength nature of migmatite and granite rocks. Bulk modulus can be used to estimate the reliability of the foundation rocks under all round pressure (Table 9)

Poisson's ratio

Poisson ratio describes the ratio of the longitudinal displacement to the axial displacement under compressive stresses. The Poisson's ratio value in the study area ranges from 0.225 to 0.320 (Figure 9). It indicates higher rate of axial displacement than the longitudinal dislocation under distressing forces that delimits the mechanical strength of the rock. Relatively low values (<0.270) were obtained

Table 8: Classification of shear modulus of the subsurface formation and their implication on the surface engineering structures.

Description	Shear Modulus (mpa)	Implication on Surface Engineering Structure (to shearing forces)
Very High	>1320	Highly Resistive
High	1090–1319	Resistive
Medium high	860–1089	Medium Resistance
Low	630–859	Yielding
Very Low	<629	Very Yielding

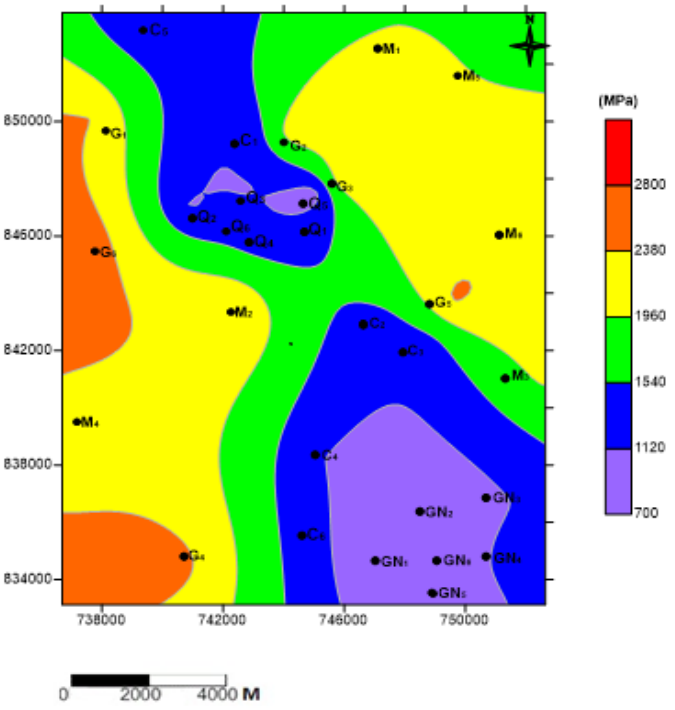

Figure 8: Bulk modulus map of the study area.

Table 9: Classification of bulk modulus of the subsurface formation and their implication on the surface engineering structures.

Description	Bulk Modulus (mpa)	Implication on Surface Structure
Very High	>2700	Sound
High	2200–2699	Good for any structure
Medium high	1700–2199	Good for any structure except large dam
Low	1200–1699	Variable
Very Low	<1200	Unreliable

in the areas underlain by quartzite, charnockite and gneiss. Relatively higher values (>0.270) characterize the area underlain by magmatic and granitic rocks. Poisson's ratio shows the strength of subsurface rock formation under the influence of the overhead prevailing stresses (Table 10).

Comparative analysis of the geophysical and mechanical results

The regression plots of the gravity and specific gravity values as

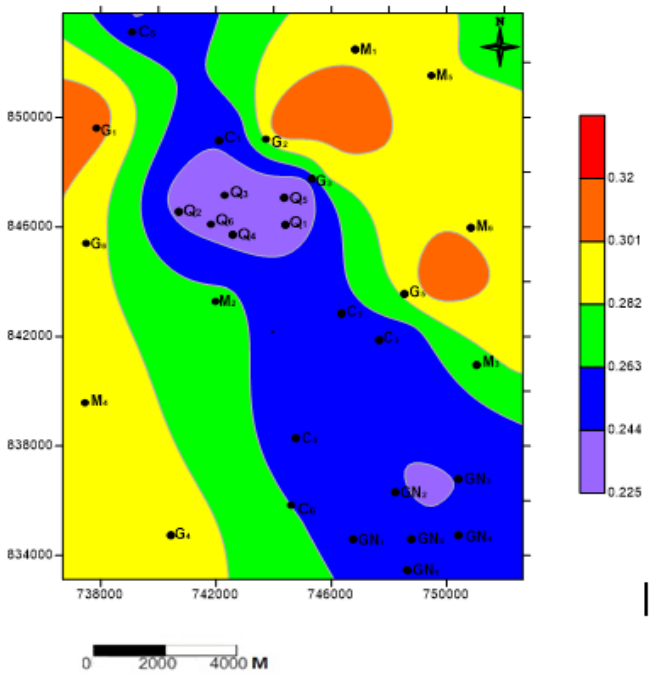

Figure 9: Poisson's ratio map of the study area.

Table 10: Classification of Poisson's ratio of the subsurface formation and their implication on the surface engineering structures.

Class	Description	Poisson's Ratio	Implication on Surface Structure
A	Very High	>0.31	Very Strong
B	High	0.29–0.30	Strong
C	Medium high	0.27–0.28	Medium Strong
D	Low	0.25–0.26	Weak
E	Very Low	< 0.24	Very Weak

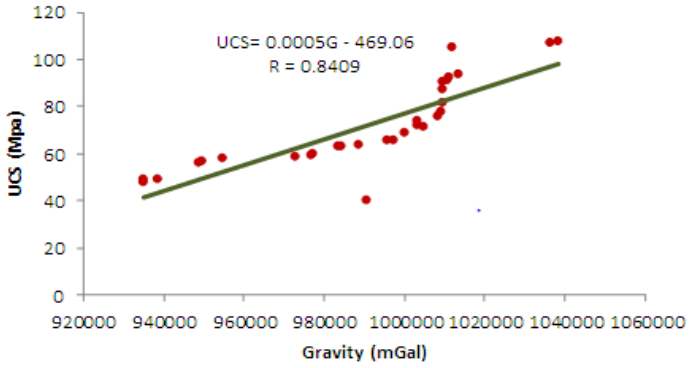

Figure 10: Crossplot of the gravity (G) and uniaxial compressive strength (UCS).

physical parameters against each of the determined mechanical parameters can be represented by an empirical equation of the form;

$$Y=MX+C \quad (15)$$

'Y' represents the mechanical parameters, 'X' represent the physical parameters, 'M' represent the gradient of the trend line, and 'C' is the intercept on the mechanical parameter (vertical) axis. From the plot, the relationship between the mechanical parameter and the physical parameters is best described by linear relationships, where

the mechanical parameter is taken as the dependent variable and the physical parameter as independent variable. i.e. the determined mechanical parameter of the rock samples varies with the physical parameter of the underlying rocks within the study area.

Relationship between the Gravity(G) and Uniaxial Compressive Strength (UCS)

The regression plot of gravity (G) against the Uniaxial Compressive Strength (UCS) of the rock samples is presented in Figure 10. The trend line with 0.84 coefficient correlation (R) show a good correlation between the gravity and the Uniaxial Compressive Strength.

The empirical equation for the relationship between Gravity and the Uniaxial Compressive Strength is given as;

$$UCS=(0.00005)G-469.06 \quad (16)$$

Where UCS=Uniaxial Compressive Strength

G=Gravity

Relationship between the Gravity(G) and Young's modulus (E)

The cross plot of gravity (G) against the Young's Modulus (E) of the rock samples is as shown in Figure 11. The trend line shows a direct relationship; which shows that, the higher the gravity of the rock, the higher the Young's Modulus of the rocks. The trend line equation for the cross plot gives coefficient of correlation (R) of 0.52 which indicates moderately good correlation between the gravity and the Young's Modulus.

The empirical equation representing the relationship between Gravity and the Young's Modulus is given as;

$$E=0.0111G-8921.6 \quad (17)$$

Where E=Young's Modulus

G=Gravity

Relationship between the Gravity(G) and Poisson's ratio (V)

The cross plot of gravity (G) against the Poisson's Ratio (**V**) of the rock samples is as presented in Figure 12. The cross plot shows a direct relationship between them, which shows that, the higher the gravity of a rock, the higher the Poisson's Ratio of the rock. The equation relating the two parameters together gives 0.76 coefficient of correlation (R), indicating relatively good relationship between the two parameters.

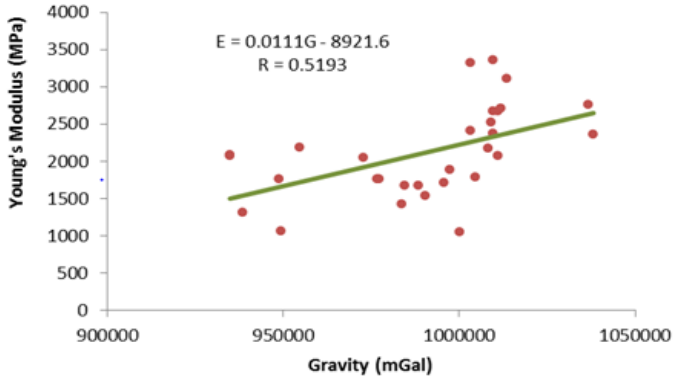

Figure 11: Crossplot of the gravity (G) and Young's modulus (E).

The empirical equation relating gravity and the Poisson's Ratio is given as;

$$V=(7 \times 10^{-7})G-0.4223 \quad (18)$$

Where **V**=Poisson's Ratio

G=Gravity

Relationship between the Gravity(G) and Shear modulus (μ)

Figure 13 shows cross plot of gravity (G) and the Shear Modulus (μ) of the rock samples. The trend line shows a direct relationship, which shows that the higher the gravity of a rock, the higher the Shear Modulus of the rocks. The trend line equation for the cross plot gives coefficient of correlation (R) equal to 0.48, indicating relatively weak correlation between the two parameters.

The empirical equation representing the relationship between gravity and the Shear Modulus is given as;

$$\mu=0.0039G-3031.7 \quad (19)$$

Where μ=Shear Modulus

G=Gravity

Relationship between the Gravity(G) and Bulk modulus (K)

The cross plot of gravity (G) against the Bulk Modulus (K) of the rock samples is as presented in Figure 14. The trend line shows a direct relationship between the two parameters with 0.72 coefficient of correllation (R) which shows that the higher the gravity of the rock, the higher the Bulk Modulus of the rocks. This indicates relatively good correlation between the gravity and the Bulk Modulus.

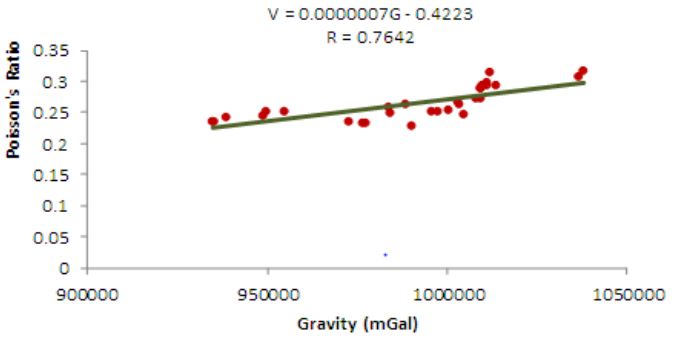

Figure 12: Crossplot of the gravity(G) and Poisson's ratio (V).

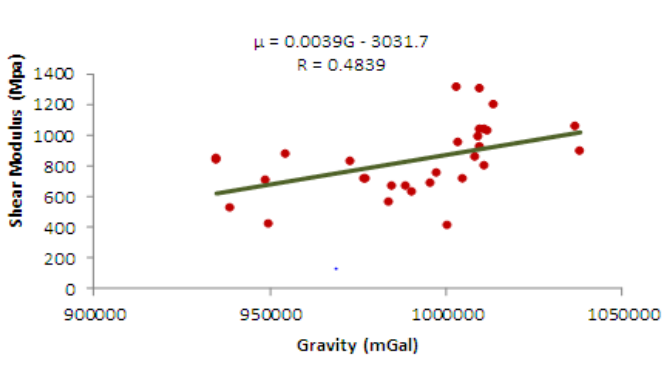

Figure 13: Crossplot of the gravity(G) and shear modulus (μ).

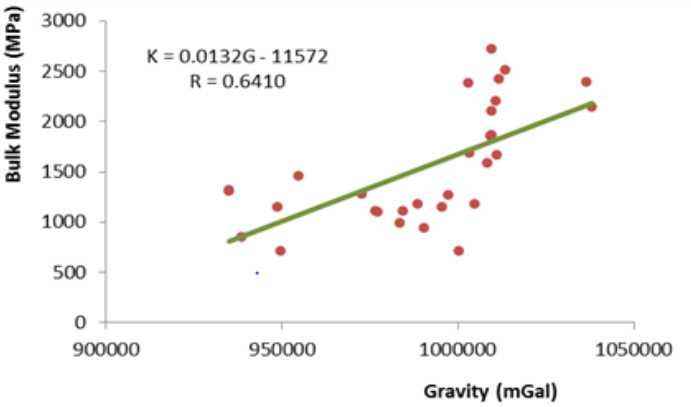

Figure 14: Crossplot of the gravity(G) and bulk modulus (μ).

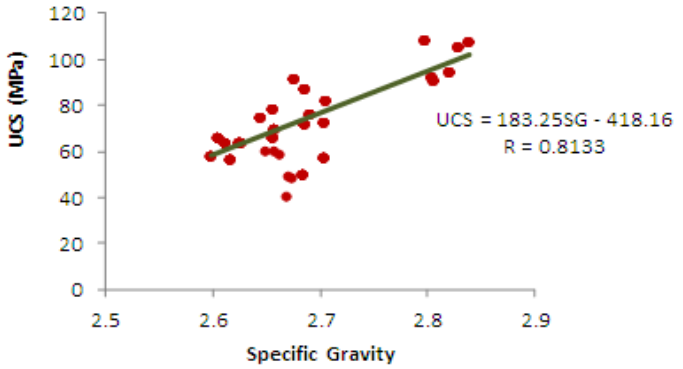

Figure 15: Crossplot of the specific gravity(SG) and uniaxial compressive strength (UCS).

The general empirical equation representing the relationship between gravity and the Bulk Modulus is given as;

K=0.0132G–11572 (20)

Where K=Bulk Modulus

G=Gravity

Relationship between the Specific Gravity(SG) and Uniaxial Compressive Strength (UCS)

Figure 15 shows a cross plot of specific gravity (G) and the Uniaxial Comressive Strength (UCS) of the rock samples. The trend shows a direct relationship, indicating that the higher the specific gravity of a rock, the higher the Uniaxial Comressive Strength of the rocks. The trend line equation for the cross plot gives coefficient of correlation (R) is equal to 0.81, indicating a relatively strong correlation between the two parameters.

The empirical equation relating specific gravity and the Uniaxial Comressive Strength is given as;

UCS=183.25SG-418.16 (21)

Where UCS=Uniaxial Compressive Strength

SG=Specific Gravity

Relationship between the Specific Gravity(SG) and Young's modulus (E)

The regression plot of specific gravity (SG) against the Young's modulus (E) of the rock samples is as presented in Figure 16. The trend line shows a direct relationship between the two parameters with 0.60 coefficient of correlation (R). This indicates a moderately good correlation between the specific gravity and the Young's modulus.

The empirical equation relating specific gravity and the Young's Modulus is given as;

E=4734.35G-10604 (22)

Where E=Young's modulus

SG=Specific Gravity

Relationship between the Specific Gravity(SG) and Bulk modulus (K)

Figure 17 shows a cross plot of specific gravity (SG) and the Bulk modulus (K) of the rock samples. The trend line shows a direct relationship, which shows that the higher the specific gravity of a rock, the higher the Bulk modulus of rocks. The trend line equation for the cross plot gives coefficient of correlation (R) equals to 0.70, indicating a very strong correlation between the two parameters.

The general empirical equation representing the relationship between specific gravity and the Bulk modulus is given as;

K=5567.8SG-133 (23)

Where K=Bulk modulus

SG=Specific Gravity

Relationship between the Specific Gravity(SG) and Shear modulus (μ)

The regression plot of specific gravity (SG) against the Shear

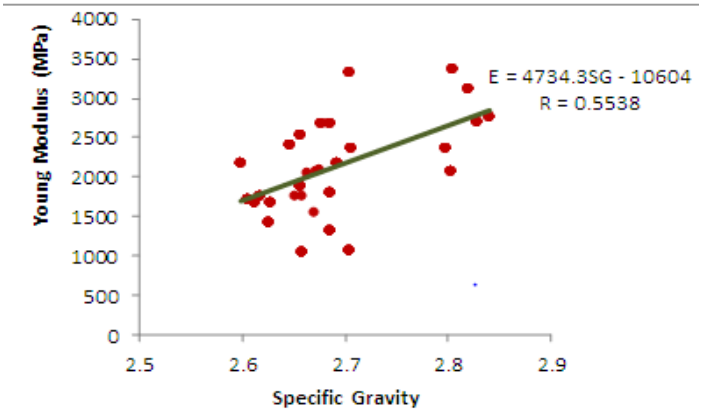

Figure 16: Crossplot of the specific gravity(SG) and Young's modulus (E).

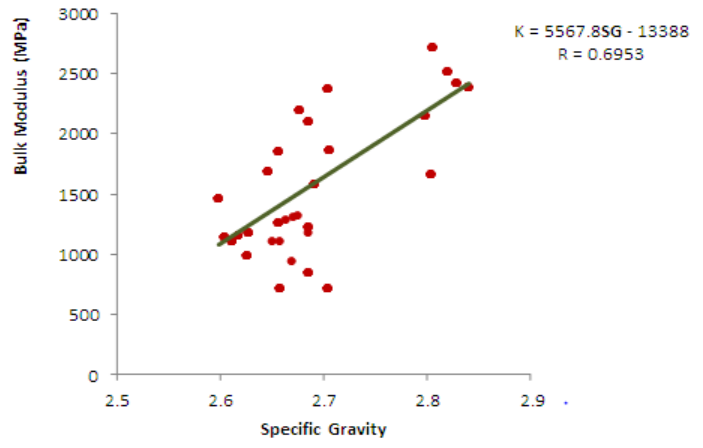

Figure 17: Crossplot of the specific gravity(SG) and bulk modulus (K).

modulus (μ) of the rock samples is presented in Figure 18. The trend line shows a direct relationship, which demonstrates that the specific gravity of the rock is directly proportional to the Shear modulus of the rocks. The two parameters have 0.52 as their coefficient of correlation (R) showing moderately good correlation between them.

The empirical equation relating specific gravity and the Shear modulus is given as;

$$\mu=1679.5SG-3681.5 \quad (24)$$

Where μ=Shear modulus

SG=Specific Gravity

Relationship between the Specific Gravity(SG) and Poisson's ratio (V)

Figure 19 shows cross plot of specific gravity (SG) and the Poisson's ratio (**V**) of the rock samples. The trend line shows a direct relationship the two parameters, with 0.81 as the coefficient of correlation (R) between them. This shows a very good correlation between the two parameters.

The empirical equation relating specific gravity and the Poisson's ratio is given as;

$$\mathbf{V}=0.2524SG-0.4098 \quad (25)$$

Where **v**=Poisson's ratio,

SG=Specific Gravity

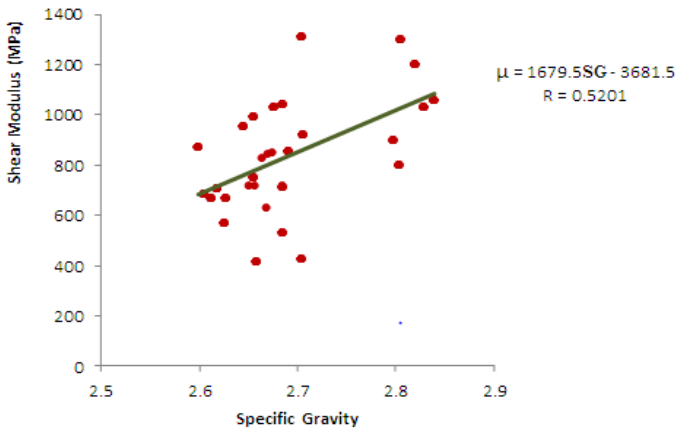

Figure 18: Crossplot of the specific gravity (SG) and shear modulus (μ).

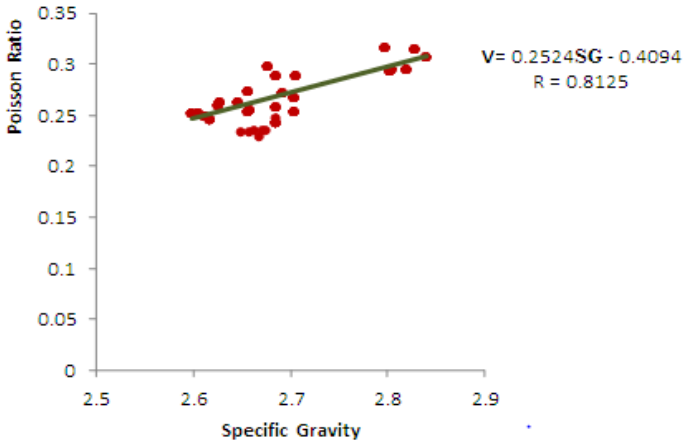

Figure 19: Crossplot of the specific gravity (SG) and Poisson's ratio (V).

Data validation

Ten samples were collected from different locations different from the initials thirty sampling points within the study area for result validation (Figure 20). Two samples from each of the five rock types (Granite, Charnockite, Migmatite, Gneiss and Quartz) were taken for the result validation analysis. The Physical parameters (gravity and specific gravity) and the mechanical parameters (Young's Modulus, Bulk Modulus, Shear Modulus, Poisson's Ratio and the Uniaxial Compressive Strength) were also determined following the same methodology earlier discussed in the study.

The physical parameters (gravity and specific gravity) obtained were computed into the empirical equations (equation 14–24) generated from the regression analysis. The predicted results obtained were compared to the observed results obtained from the laboratory analysis of the rock samples using linear regression, to check the reliability of the derived empirical equations. The errors and the percentage errors were determined from the juxtaposition.

The observed and predicted results were correlated using the relationship between gravity and the mechanical properties (Figures 21-25). The coefficient of correlation (R) (between the predicted and the observed) for Uniaxial compressive strength, Young's modulus, shear modulus, Poisson's ratio and bulk modulus are: 0.76, 0.40, 0.37, 0.78 and 0.54 respectively (Table 5) while the average percentage errors are: 25.75, 9.95, 12.23, 2.07 and 15.97 respectively (Table 6). Therefore, empirical equations gives a good representation for Uniaxial Compressive Strength and Poisson's

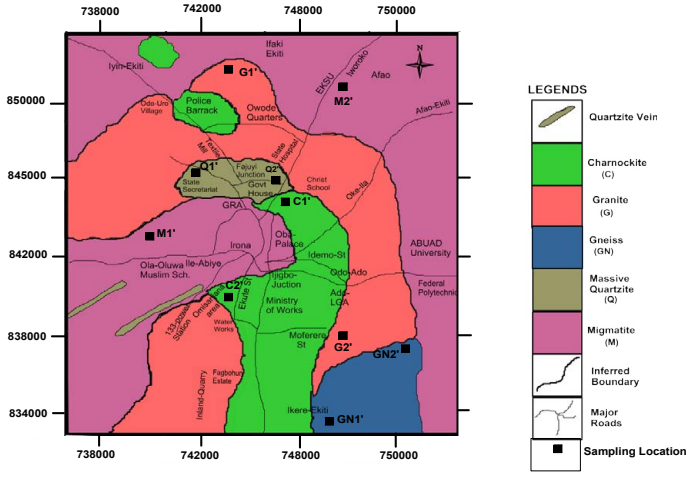

Figure 20: Geology map of the study area showing the sampling locations for the verification data.

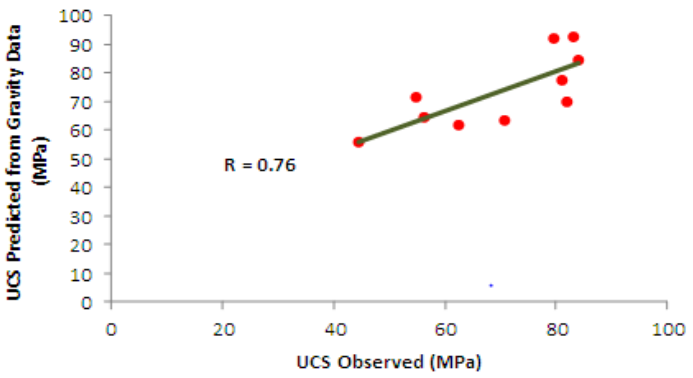

Figure 21: Cross plot of the observed and predicted results of uniaxial compressive strength from result of gravity.

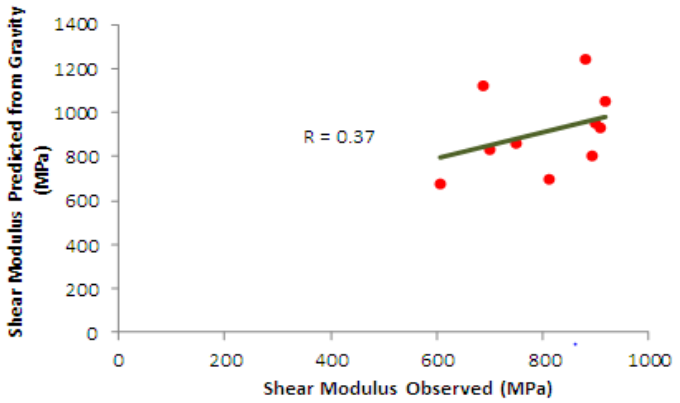

Figure 22: Cross plot of the observed and predicted results of shear modulus from result of gravity.

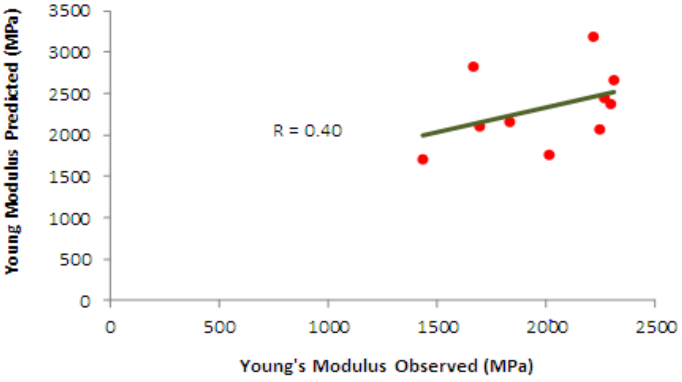

Figure 23: Cross plot of the observed and predicted results of young's modulus from result of gravity.

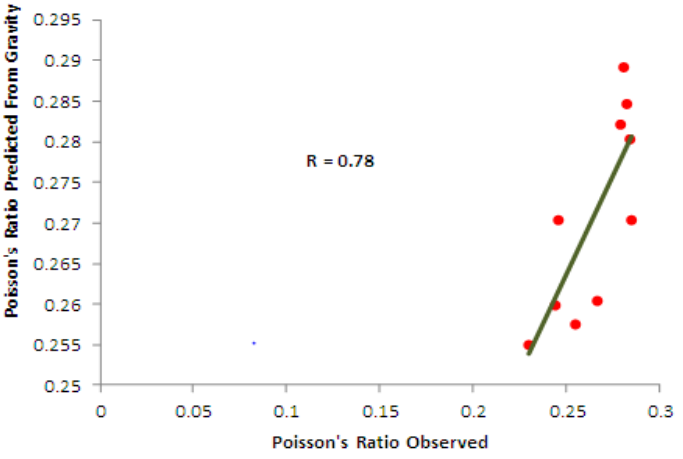

Figure 24: Cross plot of the observed and predicted results of Poisson's ratio from result of gravity.

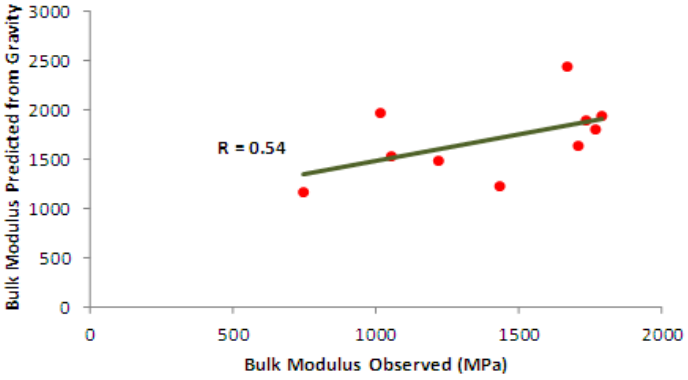

Figure 25: Cross plot of the observed and predicted results of bulk specific-gravity.

Ratio, although the percentage error is high, which may be as a result of other factors that came up during extrapolation, while weak correlation exist in the cross plots for Young's Modulus, shear modulus and bulk modulus. However, the percentage errors obtained Young's modulus is less than 10%, which is a good representation of the developed equation.

The estimated mechanical properties from the developed specific gravity empirical equations were also correlated with the observed results to show how symbolic the equations can become in generating mechanical properties (Figures 25-30). The coefficient of correlation (R) (between the predicted and the observed) for Uniaxial compressive strength, Young's modulus, shear modulus, Poisson's ratio and bulk modulus are: 0.79, 0.43, 0.41, 0.41 and 0.50 respectively (Table 5), while the average percentage errors are: 0.27, 8.02, 8.04, 1.24, and 7.51 respectively (Table 6). The coefficient of correlation reveals that only the Uniaxial Compressive Strength developed equation that has a good representation, while others has very weak correlation coefficients.

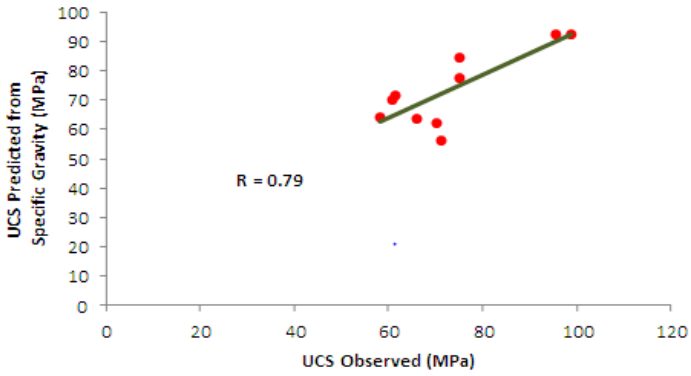

Figure 26: Cross plot of the observed and predicted results of uniaxial modulus from result of gravity.

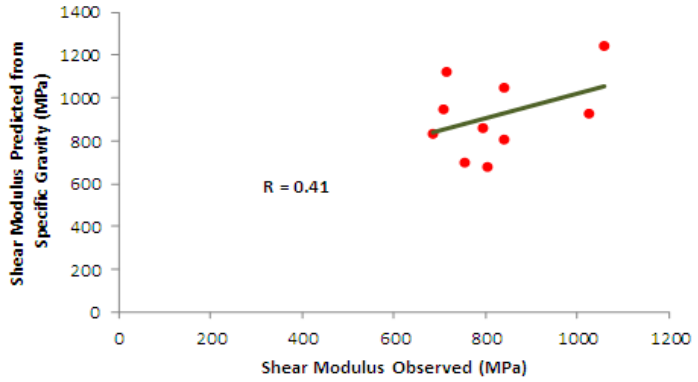

Figure 27: Cross plot of the observed and predicted results of shear.

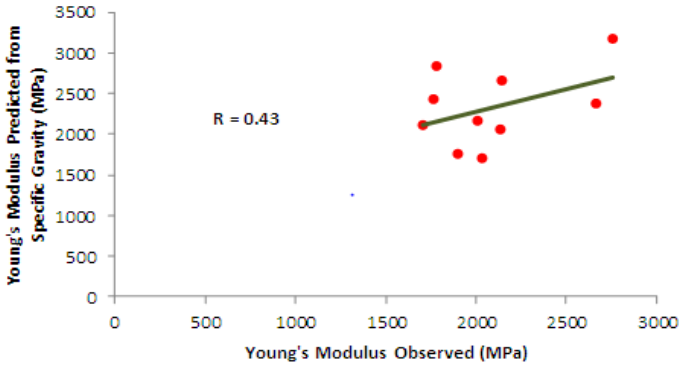

Figure 28: Cross plot of the observed and predicted results of youngs modulus from result of specific-gravity.

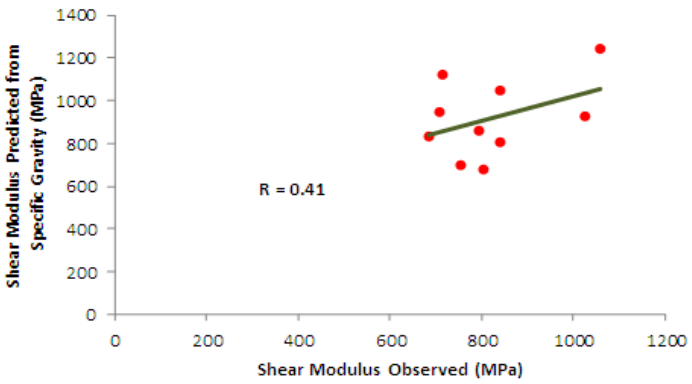

Figure 29: Cross plot of the observed and predicted results of Poisson's.

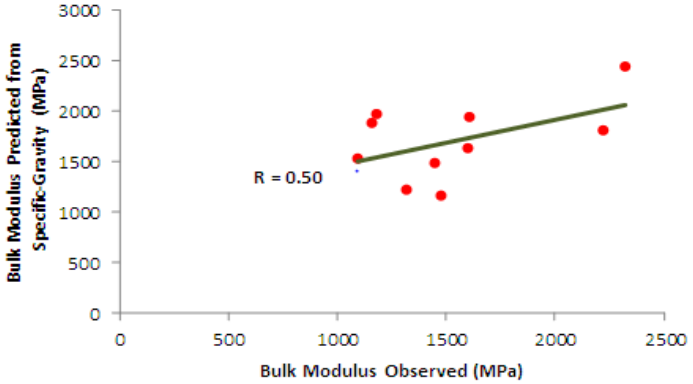

Figure 30: Cross plot of the observed and predicted results of bulk modulus from result of specific-gravity.

Table 11: Empirical equations generated from the relationships between the physical and mechanical properties of rocks.

Parameters	UCS (MPa)	Young's Modulus (MPa)	Shear Modulus (MPa)	Poisson's Ratio	Bulk Modulus (MPa)
Gravity (mGal)	UCS=(0.00005)G - 469.06	E=0.0111G – 8921.6	μ=0.0039G–3031.7	**V**=0.0000007G –0.4223	K=0.0132G – 11572
Specific Gravity	UCS=183.25SG - 418.16	E=4734.35SG –10604	μ= 1679.5SG– 3681.5	**V**= 0.2524SG–0.4098	K= 5567.8SG –13388

Table 12: Coefficients of correlation in the relationships between the physical and mechanical properties of rocks.

Parameters	UCS (MPa)	Young's Modulus (MPa)	Shear Modulus (MPa)	Poisson's Ratio	Bulk Modulus (MPa)
Gravity (m Gal)	0.8409	0.5697	0.5297	0.8546	0.7172
Specific Gravity	0.8133	0.5538	0.5201	0.8125	0.6953

Table 13: Coefficients of correlation of relationships of the predicted mechanical properties from physical investigation and the observed mechanical properties of rocks.

Parameters	UCS (MPa)	Young's Modulus (MPa)	Shear Modulus (MPa)	Poisson's Ratio	Bulk Modulus (MPa)
Gravity (mGal)	0.76	0.4	0.37	0.78	0.54
Specific Gravity	0.79	0.43	0.41	0.41	0.5

Physical and mechanical parameters of basement rocks distributed within and around parts of Ado-Ekiti, Southwestern, Nigeria were correlated with the aim of establishing empirical relationship between the two parameters. The principal Basement rocks in the study area are; Charnockite, Migmatite, Granite Gneiss and Quartzite. The largest part of the area is dominated by migmatite. The gravity values range from 935055.46 mGal to 1038167.647 mGal, while specific gravity values range from and 2.61 to 2.83. The values of Uniaxial Compressive Strength (UCS), Young's modulus (E), Shear modulus (μ), Bulk modulus (K) and Poisson's ratio (v) ranging from 49–107 MPa, 1003–3321 MPa, 416–1310 MPa,707-2728 MPa and 0.232-0.316 respectively. Migmatitic rock was observed to possess highest values of mechanical strength among the five other rock types.

The cross correlation of the gravity and specific gravity as physical parameters and all the analyzed mechanical parameters within the study area show direct relationship i.e. these mechanical parameters increases with an increase in each of the physical parameters. The cross plots of the mechanical parameters with the gravity generally show good correlation with correlation coefficient ranging from 0.52 to 0.84, except for Shear Modulus which show weak (0.50) correlation with the gravity. Good correlation were obtained in all the cross plots between the mechanical properties and the specific gravity, with coefficient of correlation (R) that ranges from 0.52 to 0.81. Since the coefficient of correlation between each of the established physical parameters and the determined mechanical properties of the basement rock in the study area are generally strong, it implies that mechanical properties of basement rocks can be estimated from physical measurements using the established empirical equations for each of the determined parameters (Tables 11 and 12). The validation exercise (correlating the observed and the predicted results supported with the results of the percentage errors) demonstrates Uniaxial Compressive Strength and Poisson's ratio have good representations in their relationships with the three geophysical parameters (Table 13).

CONCLUSION

The established relationship between the gphysical and the mechanical parameters reveals that, the mechanical strength of rock is a function of the gravitational pull effect on the rocks. Also, The study also reveal that migmatitic and granite possess more mechanical strength than the other principal rock types that characterise the study area. The areas where high rock mechanical properties were observed signify high reliability, stiffness and mechanical strength for civil engineering developments. The study is able to establish that physical properties of rocks can be used to generate mechanical properties as hypothesized from previous studies. The study is applicable in the study of the mechanical

strength of Basement rock as foundation bedrock to withstand the load to be impacted by any proposed heavy weight civil engineering structures e.g. high rising buildings, fly-over bridges, telecommunication mast, tunneling, and rail-lines. The study is applicable in any region of related geologic terrain. The generated equations from this research will help civil engineers to acquire information about any related terrain faster, cheaper and in a more comprehensive mode. Further studies can also be carried out in the area using gravimeter equipment for the geophysical gravity determination and aeromagnetic data to be correlated with mechanical properties for proper foundation studies. Also, the study can be conducted distinguishing different rock type individually.

REFERENCES

1. Folahan PI. Application of geophysical methods to building foundation studies. Int J Geosci. 2013;4:1256-1266.
2. Aina A, Olorunfemi MO, Ojo JS. An integration of aeromagnetic and electrical resistivity methods in dam site investigation. J Geophys. 1996;61:349-356.
3. Frolova J, Ladygm V, Rychagov S, Zukhubaya D. Alterations on physical and mechanical properties of rocks in the kuril-kanchata Island arc. J Eng Geol. 2012;183:80-95.
4. Bell FG. Engineering Geology. 2nd Edn, Butterworth-Heinemann, Great Britain 2007.
5. Ayodele OS, Ajayi CA. Petrology, Mineralogy and Geochemistry of the Precambrian Rocks around Ikere-Ekiti, Southwestern Nigeria. J Chem Petrochem Technol. 2016;2:1-24.
6. Rahaman MA. Review of basement geology of Southwestern Nigeria, Department of Geology, Obafemi Awolowo University, ile-ife, Osun-state Nigeria. 1979.
7. http://www.rmz-mg.com/letniki/rmz60/RMZ60_0073-0086.pdf
8. https://ui.adsabs.harvard.edu/abs/1985JAfES...3..115A/abstract
9. Talabi AO, Afolagboye OL, Ademilua OL. Physical and mechanical properties of rocks from the archean-Proterozoic terrain of Ado-Ekiti, South-Western Nigeria: Implications on its groundwater potential. Int J Adv Eng Manage Appl Sci. 2014;1:2349-3224.
10. Olarewaju VO. Charnockite-granite association in SW Nigeria: Rapakivi granite type and charnockitic plutonism in Nigeria. S AFR J Earth Sci. 1987;6:67- 68.
11. Eldosouky AM. Integration of remote sensing and aeromagnetic data for mapping structural features and hydrothermal alterations zones in Wadi Allaqi area, south eastern desert of Egypt. J Earth Sci. 2017;130:28–37.
12. Eldosouky AM, Elkhateeb SO. Texture analysis of aeromagnetic data for enhancing geologic features using co-occurrence matrices in Elallaqi area, south-eastern desert of Egypt. Nriag J Astron Geophy. 2017:2090-9977.
13. https://core.ac.uk/download/pdf/21747136.pdf
14. Hao Z, Wen Z, Runcheng X, Lina D, Christopher X, Yuming S, et al. Characterization of rock mechanical properties using lab tests and numerical interpretation model of well logs. Math Probl Eng. 2016;1:1155.
15. Telford WM. Applied geophysics. 2nd Edn, Cambridge University Press, Cambridge, New York, Port Chester Melbourne Sydney 1990.